Renewable Energy 228 (2024) 120577

Contents lists available at ScienceDirect

Renewable Energy

journal homepage: www.elsevier.com/locate/renene

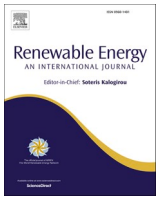

Analysis and prediction of the performance and reliability of PV modules installed in harsh climates: Case study Iraq

Mohammed Adnan Hameed [a,b,c,*], Ismail Kaaya [d,e,f], Mudhafar Al-Jbori [g], Qais Matti [h], Roland Scheer [a], Ralph Gottschalg [c]

[a] Martin-Luther-University Halle-Wittenberg, Halle, Germany
[b] Ministry of Oil -SCOP, Baghdad, Iraq
[c] Fraunhofer Center for Silicon Photovoltaics CSP, Halle, Germany
[d] Imec imo-imomec, Thor Park 8320, Genk, Belgium
[e] EnergyVille imo-imomec, Thor Park 8320, Genk, Belgium
[f] Hasselt University imo-imomec, Hasselt, Belgium
[g] Representative of Iraq in IRENA, Iraq
[h] Retiered Faculty Member in the University of Technology, Baghdad, Iraq

ARTICLE INFO

Keywords:
Degradation rate
Energy yield
Harsh climate
Lifetime
Prediction
PV modules
Iraq

ABSTRACT

The increasing global demand for renewable energy necessitates a comprehensive understanding of solar photovoltaic (PV) system performance and reliability, particularly in harsh climates such as Iraq. Despite ambitious targets to diversify its energy sector, Iraq faces challenges in the deployment of PV projects due to limited field experience. In this study, we assess the reliability and performance of two different PV systems installed in Basrah and Baghdad, aged 3.5 and 8 years, respectively. Field analysis reveals prevalent issues including glass and cell breakage, delamination, solder bond fatigue, and encapsulant discoloration, contributing to medium degradation rates of 0.91 %/year and 2.6 %/year in Basrah and Baghdad, respectively. Our investigation attributes higher degradation rates not only to ageing but also to suboptimal operation and maintenance (O&M) practices. Additionally, since the two systems are from different manufacturers, we verify that the measured higher degradation rates are mainly attributed to harsh operating conditions rather than differences in manufacturing processes. To extrapolate our findings countrywide, we employ a physics-based model to simulate the degradation rates. Based on the simulated degradation, we proposed four degradation rate zones across the country with degradation rates ranging from 0.62 %/year to 0.96 %/year. By applying these rates to estimate lifetime energy yield across different zones, we demonstrate the trade-offs between higher irradiance zones with reduced PV lifetime and low irradiance zones with longer PV lifetimes. In the study, we compared energy yield simulations using fixed degradation rates with those employing climate-dependent degradation rates. Our analysis revealed that in certain locations in Iraq, employing a fixed degradation rate underestimates the yield by approximately 9.7 %. Conversely, in other locations, it results in overestimations ranging from approximately 10.5 %–31.1 %, highlighting the importance of accurate degradation rate modelling for PV system assessment. Furthermore, we simulate the impact of soiling losses on energy yield, revealing potential losses of up to 70 % depending on location and cleaning schedules. Our findings contribute valuable insights into PV system degradation across harsh climates, addressing critical gaps in global degradation rate data and facilitating more accurate climate-dependent assessments of PV performance and reliability.

1. Introduction

Iraq is one of OPEC's largest crude oil producers, with 17 % of Middle Eastern oil proven reserves and 8 % of global reserves [1]. Its production by 2030 is set to be the third largest contributor to global oil supply [2]. Currently, the country's electricity sector is almost entirely dependent on fossil fuels, which account for more than 80 % of power generation [3]. Iraq also holds strong solar PV potential because of its strategic

* Corresponding author. Martin-Luther-University Halle-Wittenberg, Halle, Germany.
E-mail address: m.adnan.scop@gmail.com (M.A. Hameed).

https://doi.org/10.1016/j.renene.2024.120577
Received 27 September 2023; Received in revised form 27 March 2024; Accepted 27 April 2024
Available online 27 April 2024

location with large amounts of incident solar radiation more than 3000 h of bright sunshine per year, with average daily sunshine of 11–12 h in summer and 7–8 h in winter. However, despite its vast energy resources, the electricity sector in Iraq is experiencing shortages and a series of power outages hindering the country's economic development.

In the quest to improve its electricity sector, the country's energy sector has set great ambitions to diversify its energy mix by increasing its renewable energy capacity. For example, Iraq has an ambition to have an installed solar generation capacity of 10 GW by 2030, representing 20–25 % of its energy mix to reduce its carbon footprint and its reliance on fossil fuel-based power generators [4]. The country has already signed some deals with international companies such as TotalEnergies to build a 1 GW solar plant and with both PowerChina and Masdar to build PV plants totalling 4 GW as it seeks to achieve its renewables ambitions [4].

Despite these efforts, Iraq's PV sector faces notable challenges, particularly in terms of reliability and performance. The country's harsh climate, characterized by extreme temperatures, high irradiance, wide differences in temperature intraday, and frequent sand and dust storms, poses significant obstacles to PV system durability and efficiency [5–8]. Degradation processes originate from how PV modules and their materials interact with the environment, leading to varied degradation rates and lifetimes across locations. Climate and technological variations in degradation rates have been reported in numerous studies [5,9–18] which demonstrate an increasing interest to evaluate PV module reliability across different climates. The motivations of these studies are mainly driven by research and financial aspects. In the research aspect, the aim is to improve PV module technology and Bill of Materials (BoM) durability applicable in various climates. Financially, PV installers seek to minimize uncertainties in PV project's bankability by adjusting degradation rates depending on climates. Although previous studies have examined the degradation rates and failure patterns in various regions, countries, or climate zones, the degradation rates and failure modes in many areas with significant potential for solar PV generation, such as Iraq, remain undocumented.

While existing literature has extensively evaluated Iraq's solar PV potential [7,19,20], and identified performance degradation due to soiling [21–23], there remains a critical gap in understanding long-term reliability aspects, including degradation by age or the combined effects of soiling and age-related degradation.

The novelty of this study lies in addressing these research gaps by focusing on the following objectives:

- o Firstly, we address the gap of undocumented field degradation of PV modules in Iraq by analyzing the degradation of operational PV modules in Basrah and Baghdad that have been under field exposure for a period of 3 and 8 years respectively.
- o Secondly, we employ degradation rate and soiling loss models to simulate degradation rates and lifetime energy yield for PV modules across Iraq. Based on these simulations we propose four degradation rate zones considering the diverse climatic conditions prevalent in different parts of the country.

By adopting a methodology combining field analysis and empirical physics-based modelling, we aim to provide a holistic understanding of the factors influencing PV system performance and reliability in Iraq. In the paper, we also assess the trade-offs in lifetime energy productions among these four degradation rate zones. To the best of the author's knowledge, such a study has not been reported before.

Furthermore, despite evidence suggesting variations in degradation rates based on climate conditions [5,14,17,24] 25] [25], PV manufacturers have been reluctant to implement climate-dependent performance degradation warranties. This discrepancy highlights the need for comprehensive global assessments of PV module degradation rates to provide manufacturers with concrete evidence for differentiating degradation rates across various climate zones. Therefore, this study contributes to this ongoing effort by assessing and predicting the degradation rates of PV modules installed in Iraq.

We have organized the manuscript to first describe the general introduction in section 1 where we also highlight the novelty of our study in comparison with existing studies. The other part of the introduction aims to provide a general overview of energy yield, degradation rate, and soiling loss predictions. Readers with knowledge of these topics can go directly to subsection 1.2 regarding data requirements and sources. The second section 2, describes the general methodology used to conduct this study. In section 3, we present the results and discussion of our study and finally, section 4, provides a summary conclusion of the study.

1.1. Overview of degradation and energy yield prediction

1.1.1. Degradation rate prediction due to ageing

In terms of PV performance, degradation refers to the decline or loss of PV performance over time. Degradation can be reversible (e.g., degradation caused by soiling, which can be reversed by cleaning the modules) or irreversible (e.g., degradation caused by ageing often associated with failure modes such as corrosion, cell cracks, interconnection adhesion, PV discoloration etc).

The rate at which PV modules degrade depends on many factors including the bill of materials (BoM), the PV technology, the operating climate conditions as well as the installation designs. A combination of different stress factors, PV technology and BoM, induce different degradation modes/mechanisms on the PV modules [26]. This implies that the degradation rates vary depending on the location, the BoM and the PV technology as already mentioned in Refs. [5,27,28–31].

1.1.2. Energy yield prediction

The prediction of photovoltaic (PV) energy yield plays a vital role in optimizing the performance and profitability of solar power systems. Accurate energy yield predictions enable effective decision-making regarding system design, operation, and maintenance, leading to enhanced efficiency and cost-effectiveness. Several factors influence the energy yield of PV systems. These include solar irradiance, ambient temperature, shading effects, soiling, module degradation, and electrical losses. Accurate modelling and prediction of these factors are crucial for estimating the actual energy output of PV installations. For more accurate yield estimations, a detailed three-dimensional (3D) modelling of the PV system layout, and technical specifications of plant components are required. Some sophisticated software packages such as PVSyst [26], PV*SOL [28], and others are commonly utilized to consider most of these requirements for accurate modelling and analysis of PV energy yield.

In general, the main steps required for energy yield prediction are modelled or measured environmental data, modelling the irradiance incident on the tilted PV, modelling the PV performance under varying irradiance and temperatures, applying systems losses (e.g soiling, degradation, inverter etc.), and applying statistical analysis to assess the related uncertainty [29]. A detailed assessment of the uncertainties related to PV energy yield can be found in these IEA reports [30,31]. In this paper, we focus on assessing the variations in lifetime energy yield prediction based on PV degradation due to ageing and degradation by reversible effects such as soiling.

Different modelling approaches are available for the energy yield prediction as discussed in Ref. [32]. These methods can be categorized as:

Physics-based methods: These methods incorporate fundamental equations describing the behaviour of PV cells, considering electrical characteristics, module design, and environmental factors [33]. Numerical simulations based on these models enable energy production prediction under specific conditions. Physics-based methods are preferred due to their capacity for a physical interpretation of predicted results. However, they often require extensive computational resources

and numerous physical input parameters which are not usually available.

Statistical and Machine Learning Methods: Statistical and machine learning methods offer an alternative approach to PV energy yield prediction. These techniques utilize historical data from operational PV systems to build predictive models. Commonly used methods in this domain include multiple regression analysis, artificial neural networks, support vector regression, and random forests [34]. These models leverage historical energy production data, weather patterns, and system parameters to forecast future energy yield.

Empirical Approaches: These techniques are typically derived from numerical fitting, where the power output is obtained by fitting a function of total irradiance and/or module temperature. They can be as simple as a matrix of irradiances multiplied by a device descriptor matrix measured either in the laboratory or outdoors for a set of known conditions [35].

1.1.3. Soiling loss prediction

Soiling is the accumulation of dirt, dust, and organic/inorganic contaminants deposited on the surface of PV modules. Soiling reduces the light intensity reaching the PV cell, by reflecting, absorbing, and scattering part of the irradiance incident on the PV module [36]. This results in a reduction of the total energy output of the PV module. Unfortunately, soiling is a significant and frequent climate challenge for PV installations in higher irradiance regions like Iraq. This is due to the high concentration of particles in the air, periodic dust storms and limited rainfalls in these regions [37]. Moreover, in Ref. [38], the authors showed that Iraq has the highest soiling loss by month with a maximum record of 65 % in the MENA region due to frequent sandstorms in Iraq. For lifetime energy predictions, addressing soiling losses adequately reduces the uncertainties in PV project financial estimations hence minimizing risks of the PV investments.

Degradation by soiling can depend on different factors such as PV module design (i.e., modules with and without anti-soiling coatings), PV installation designs (i.e., more soiling for low tilt PV modules), location (i.e., the dust particles differ from location to location and the amount of rainfall is different from one location to another). Therefore, when predicting the soiling loss rates, these aspects need to be considered. Different authors have proposed models that consider some of these aspects [39,40].

1.2. Data requirements and sources

For this study, we used both field data for field degradation analysis and publicly available data sources for degradation rate, soiling loss, and energy yield estimations.

- o To estimate the degradation rates across Iraq, processed and validated data as outlined in Ref. [27] was used as input to the physical models. These data are from ERA5 re-analysis [41] and represent the annual mean/sum for the years 2017 and 2018. Fig. 1, depicts the essential data for the degradation rate models and their variations across different regions of Iraq.
- o For the analysis of lifetime energy yield data from PVGIS [42] were utilized. Time series spanning from 2005 to 2020 were used for energy yield evaluations. The process of data extraction is depicted in Fig. 2.
- o Rainfall data were also extracted from Copernicus Climate Change Service [43] in daily averages. Fifteen years of time series from 2005 to 2020 were extracted to align with the data used for energy yield prediction.
- o For field degradation analysis, two operational PV systems in Iraq were selected as case studies to identify the most common degradation/failure modes and to evaluate the degradation of electrical parameters. The first plant is located in Baghdad and comprises modules of 8 years at the time of the investigation. These modules are multi (Poly) crystalline from SHARP ND-F210AI and are glass-backsheet modules. The second plant investigated is located in Basrah about 570 km south of Baghdad. At the time of visual inspection, the modules were 2 years old. They were electrically investigated after 3.5 years of installation. The modules are also multi (Poly) crystalline and glass-back sheet modules but from a different manufacturer from those in Baghdad. The datasheet specifications of the modules are provided in Table 1. The decision to utilize these systems was primarily based on the accessibility as they are owned by the Iraq Ministry of Oil.

2. Methodology

2.1. Degradation evaluation of operational PV systems

Two PV systems located in Baghdad and Basrah, Iraq were investigated. The details of these systems are provided in subsection 1.2. Visual inspection was conducted in the field to detect any visual defects on the PV modules. During the inspection, each module was illuminated with not less than 1000 lux. For electrical degradation analysis, nine modules – three from Baghdad and five from Basrah – were disconnected and taken to the laboratory for electrical characterization under standard testing conditions (STC) at Fraunhofer CSP/Germany. Additionally, indoor electroluminescence imaging was performed to identify and correlate more potential failure modes in addition to those observed during visual inspection. The decision to conduct indoor characterization was to ensure comparable testing conditions with the datasheet, enabling the use of datasheet values for calculating the degradation rates.

To evaluate the total percentage degradation and the annual degradation rate of a given electrical parameter X (where X represent Pmax, Vmax, Imax, Voc, Isc), the following expressions were employed respectively:

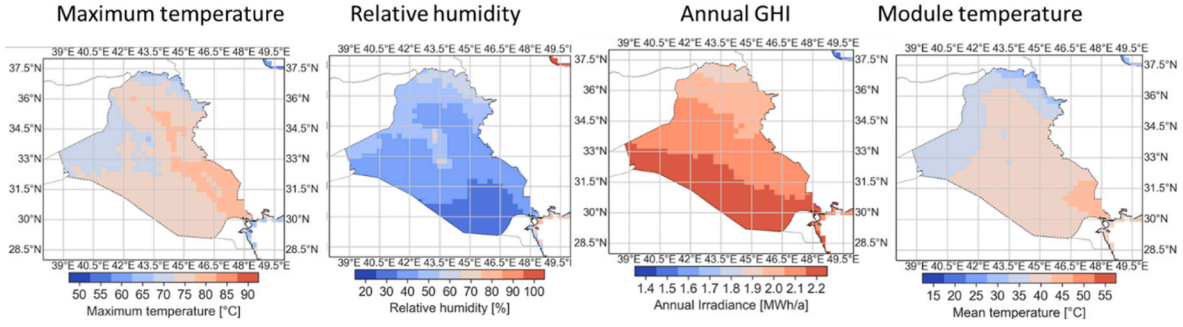

Fig. 1. Maps showing the annual mean of maximum temperature, relative humidity, module temperature and annual sum of global horizontal irradiance used as input to calculate the degradation rates.

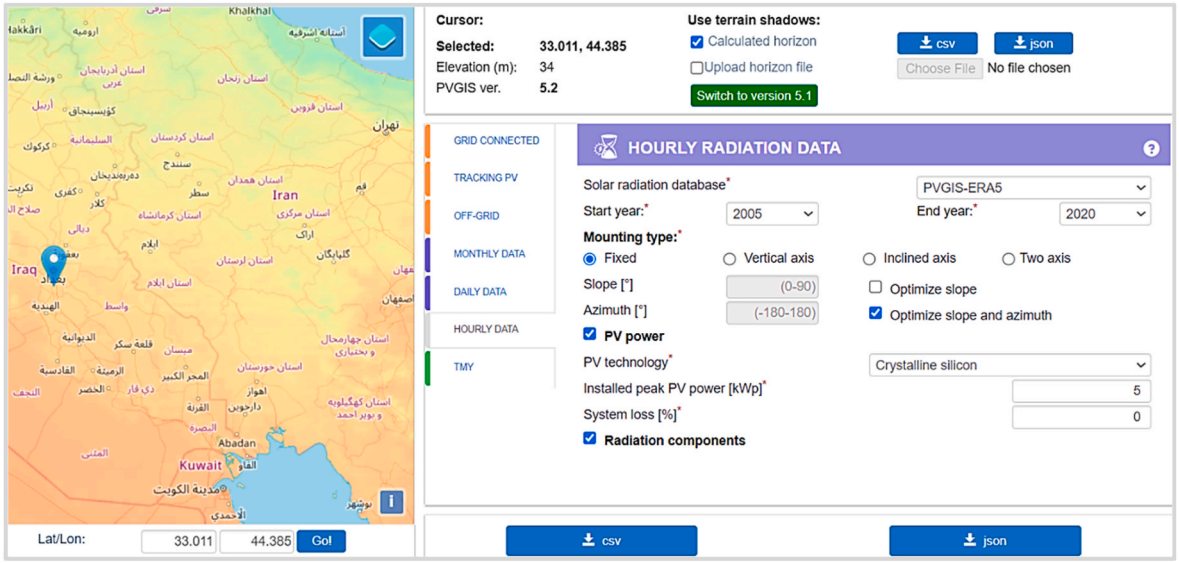

Fig. 2. Snapshot showing the selected input variables used in the simulation (similar inputs are selected for all the locations). Figure from PV-GIS [44].

Table 1
Technical data of PV modules assessed in Baghdad and Basra.

Datasheet values	Baghdad	Basrah
Maximum power (Pmax)	210.00 Wp	255.00 Wp
Open circuit voltage (Voc)	36.60 V	37.85 V
Short circuit current (Isc)	7.68 A	9.08 A
Voltage at maximum power (Vmax)	30.10 V	29.90 V
Current at maximum power (Imax)	6.98 A	8.53 A

$$\mathrm{D(X)[\%]} = \left(1 - \frac{X_2}{X_1}\right) \bullet 100 \tag{1}$$

$$\mathrm{R(X)[\%\,/\,year]} = \left(\frac{D(X)[\%]}{t_{field}}\right) \tag{2}$$

where X_2 represents the value of each electrical parameter measured in the lab at current time and X_1 represents the value of each parameter given on the datasheet. t_{field} is the time in years that the module has been exposed in the field.

2.2. Degradation rate prediction due to ageing

To evaluate the non-reversible degradation rate, we utilized the model proposed in Ref. [45]. We selected this model due to its capability to evaluate individual degradation mechanisms and its demonstrated reduced uncertainties as indicated in Ref. [46]. The total degradation rate of power (DR_T [%/year]) is estimated as a function of specific degradation mechanisms/processes based on the applied climatic stresses as [45]:

$$DR_T = A_N \cdot (1 + \mathrm{DR_H})(1 + \mathrm{DR_P})(1 + DR_{Tm}) - 1 \tag{3}$$

Where DR_H, DR_P and DR_{Tm} are the degradation rates for hydrolysis, photodegradation, and thermomechanical degradation, respectively. These rates are evaluated as functions of environmental stressors as [45,47]:

$$\mathrm{DR_H(T, RH)} = \mathrm{A_H} \cdot \exp\left(\frac{-\mathrm{E_{aH}}}{\mathrm{k_B \cdot T}}\right) \cdot \mathrm{RH^n} \tag{4}$$

$$\mathrm{DR_P(UV, T, RH)} = \mathrm{A_p \cdot UV^y} \bullet (1 + \mathrm{RH^{n_1}}) \bullet \exp\left(\frac{-\mathrm{E_{aP}}}{\mathrm{k_B \cdot T}}\right) \tag{5}$$

$$\mathrm{DR_{Tm}(\Delta T, T_{max})} = \mathrm{A_T} \cdot (\Delta T + 273)^{x} \cdot \mathrm{C_r} \cdot \exp\left(\frac{-\mathrm{E_{aT}}}{\mathrm{k_B \cdot T_{max}}}\right) \tag{6}$$

Here, k_B (8.62×10^{-5} eV/K) is the Boltzmann constant, T [Kelvin] annual average module temperature, T_{max} [Kelvin] is the annual average maximum temperature of the module, ΔT is the annual average cyclic temperature of the module, UV [kWh/m^2] is the total annual UV dose, RH [%] annual average relative humidity, C_r [cycles/year] annual temperature cycling frequency (assumed as I cycle per year). Definitions of other model parameters and values used are presented in Table 2 below.

Because the models depend on many unknown parameters that need to be extracted for a given PV module under evaluation [45] and considering that the model can have different solutions due to its exponential nature of the independent functions. By identifying the most sensitive parameter (in this case the activation energies), one can fix other model parameters and vary the activation energy to model the differences in the robustness of the PV modules. In this study, we used a non-central F distribution continuous random variable generator [48] to generate a distribution of activation energies for the difference degradation mechanisms models. This approach facilitated a form of Monte Carlo simulation, wherein we utilized over 1000 activation energies to compute the mean degradation rate.

2.3. PV power simulation

In this work, we deployed PVGIS software [49] to calculate the PV power output, mainly because it fits the scope of the study and is a widely used simulation tool in the PV community. In PVGIS, the PV power output is calculated using an empirical model described in

Table 2
Definition of model parameters and values used in degradation rate simulation.

Parameter	Quantity
A_N normalization constant of the physical quantities	1 $year^{-2}$
A_H exponential coefficient for hydrolysis	4.91$e7$ $year^{-1}$
A_P exponential coefficient for photodegradation	7.3$e7$ $(kWh/m^2)^{-1}$
A_T- exponential coefficient for thermomechanical degradation	2.04 $cycle^{-1}$
E_{aH}, E_{aP} and E_{aT} [eV] activation energies, n, n_1, y and x are model parameters that describe the effect of RH	Simulated as a distribution $n = 1.9$, $n_1 = 0.1$, $y = 0.63$ and $x = 2.04$

Ref. [50], The power is assumed to depend on irradiance G and module temperature Tm in the following way:

$$P = \frac{G}{1000} \bullet A \bullet \left(1 + k_1 \ln(G') + k_2 \ln(G')^2 + k_3 T_m' + k_4 T_m' \ln(G) + k_5 T_m' \ln(G')^2 + k_6 T_m'^2\right) \quad (7)$$

$$G' = \frac{G}{1000} \text{ and } T_m' = T_m - 25^0 \quad (8)$$

Where the coefficients k_1 to k_6 are found for each PV technology by fitting to measured data. The coefficients used in PVGIS are described in Ref. [42].

It should be noted that here, G represents the global plane of array irradiance and is estimated in PVGIS from the irradiance values on the horizontal plane of global and diffuse and/or beam irradiance components using Muneer's model [51] as the sum of the beam and diffuse components on tilted surfaces.

The module temperature is estimated from ambient temperature, plane of array irradiance and wind speed using the Faiman models [52] as:

$$T_m = T_a + \frac{G}{U_0 + U_1 \bullet WS} \quad (9)$$

Here, T_a [°C] is the air temperature, WS [m/s] is the wind speed, U_0 [W/m^2/°C] and U_1 [Ws/m^3/°C] are the coefficients describing the effect of the radiation on the module temperature and the cooling by the wind. Typical values reported for c-Si PV modules in the open-rack mounting configuration [53] (i.e. $U_0 = 26.9$ and $U_1 = 6.2$) are used in PVGIS.

In this study, a 5000 Wp PV system with crystalline silicon PV module technology has been assumed. Note that according to the scope of the study, the system or module capacity is not a determining factor since the metrics employed in the analysis, such as specific yield and PR, are independent of system size. Furthermore, although we simulated a system level, it is assumed that the only system losses are due to PV module degradation since it's the objective of our study. Fifteen years of power and irradiance data were extracted from PVGIS software by selecting the inputs as shown in Fig. 2. Note that optimal azimuth and tilt angles were applied for simulated locations by selecting optimizing slope and azimuth. To simulate long-term power, the 15 years of data is repeated and concatenated into a multi-year time series. Moreover, it has already been demonstrated that this is a viable method when long-time timeseries is available to capture year-to-year climate variability [54].

2.4. Soiling loss prediction

In this study, the Kimber soiling model [40] implemented in PVlib [55] and openly available on GitHub [56] is used to evaluate the energy losses due to soiling. The model was chosen because it enables the simulation of both manual and natural cleaning scenarios, as well as the flexibility to adjust soiling rates, which aligns with the objectives of this study. The model assumes that soiling builds up at a constant rate until cleaned either manually or by rain. The rain must reach a threshold to clean the panels. When rains exceed the threshold, it's assumed the earth is damp for a grace period before it begins to soil again. The model also assumes that there is a maximum soiling build-up that cannot be exceeded even if there is no rainfall or manual cleaning. In this study, we assumed the following input values as shown in Table 3. The soiling rates are assumed based on the reported rates in Iraq or MENA regions [38,57]. The effectiveness of the cleaning by rain varies with rainfall intensity and the length of a dry period. Indeed, in literature, different threshold of rainfall intensities from 2 mm to 20 mm have been reported as needed to entirely clean the PV systems [57]. In this paper, we have assumed the maximum threshold of 20 mm as the requirement to completely clean the PV modules. We set the grace period at 10 days, assuming that the maximum rainfall threshold would ensure sufficient dampness in the ground during this time.

Table 3
Input quantities used in simulating soiling degradation using the Kimber soiling model.

Required input	Quantity
Cleaning threshold	20 mm
Grace period	10 days
Maximum fraction of energy lost due to soiling	0.8 [-]
Soiling loss rate	0.2 %/day – 0.5 %/day (with 0.1 step)
Manual wash dates	1month – 6months (with 1-month step)

2.5. Lifetime energy yield prediction

The lifetime energy yield was evaluated considering both irreversible and reversible degradation effects. First the non-reversible degradation rate (DR) is estimated as a function of environmental stresses as described in section 2.2 and the power with degradation is estimated using a linear function as:

$$P_t\,[W] = P_{in}(1 - DR * t) \quad (10)$$

where $P_t\,[W]$ is the power at a given time with degradation, P_{in} is the initial power without degradation.

Although, we are aware of some studies describing non-linearity in degradation rates [32,58,59], a linear function and a constant degradation rate were assumed for simplicity and because it is what usually is offered by the manufacturers.

Second, the reversible degradation due to soiling was applied to the power $P_t\,[W]$ using an open-source soiling model described in section 2.4

The lifetime energy yield ($yield_{FT}$) in kWh is then estimated simply as:

$$yield_{FT} = \frac{1}{1000} \bullet \sum_{t=0}^{t=FT} P_t\,[W] \quad (11)$$

Where t is the time in hours and FT is the failure time (number of hours until defined failure of a PV module). The division by 1000 is to convert from W to kW.

2.6. Performance and statistical metrics

Two performance metrics; the performance ratio (PR) and the specific yield have been used in this study. We used the percentage change as a statistical metric for benchmarking purposes.

2.6.1. Performance ratio

PR is a metric commonly used to quantify and benchmark PV systems performance. It is expressed as a ratio or in percentage hence it is independent of plant capacity or solar resource. The PR is defined in IEC 61724 [43] as a measure of how effectively the plant converts sunlight collected by the PV panels relative to what would be expected from the panel nameplate rating. The PR quantifies the overall effect of system losses on the rated capacity, including losses caused by modules, temperature, low light efficiency reduction, inverters, cabling, shading, and soiling. For long-term PV performance degradation analysis, the temperature-corrected performance ratio is used as [60];

$$PR = \frac{P_{MPP}}{P_{STC} \bullet \frac{G_{poa}}{1000} \bullet [1 + \gamma \bullet (T_m - 25)]} \quad (12)$$

where P_{MPP} is the module or system power at maximum power point (MPP), P_{STC} is the rated module or system power at standard testing conditions (STC), G_{poa} is the plane of array irradiance, γ is the MPP temperature coefficient based on the manufacturer's specifications, T_m is the measured module temperature. The PR is calculated at each timestamp and then aggregated into daily, weekly, monthly, or yearly PR based on an insolation-weighted average.

2.6.2. Specific yield

The specific yield (kWh/kWp) is the total energy (kWh) generated per kWp installed capacity over a fixed period. In other terms, the specific is the measure of the number of hours a plant produced during a specific period. Specific yield parameter normalizes plant output over a chosen period and thus allow the comparison of the production of plants with different power plants or even different power production technologies. It is often used to determine the financial value of a plant and compare operating results from different technologies and systems. In this study, the annual specific yield was used to compare the performance of modules in separate locations as:

$$\text{Annual specific yield}\left(\frac{\text{kWh}}{\text{kW}_\text{p}}\right) = \frac{\text{Annual yield}}{\textit{Installed PV capacity}} \tag{13}$$

2.6.3. Percentage change

A percentage change is a way to express a change in a variable. It represents the relative change between the old value and the new one [61]. It is expressed as:

$$\text{Percentage change}\ (\%) = 100 \bullet \frac{Y_2 - Y_1}{Y_1} \tag{14}$$

Where Y_1 is the fixed reference value and Y_2 is the varying new value.

3. Results and discussion

3.1. Analysis and prediction of PV module degradation

In this section, we present the results from visual inspection, performance, and EL characterization of the two systems in Baghdad and Basrah.

3.1.1. Visual inspection

Table 4, presents the failure modes observed during visual inspection for both systems across the two locations. Additionally, Fig. 3 shows the snapshots of the visible failure modes. Notably, the list of failure modes in Baghdad is exhaustive compared to Basrah, this is expected because the modules analyzed in Baghdad are much older than those in Basrah (i.e., 8 years compared to 2 years in Basrah). However, a common observation is that both modules experienced delamination of either the backsheet or the front encapsulant. This could be attributed to quality issues – manufacturing defects or natural degradation due to thermo-mechanical stresses or exposure to higher UV doses. Furthermore, this aligns with the findings of authors in Ref. [62], who also noted delamination as a prevalent failure mode for PV modules operating in harsh climate conditions characterized by elevated UV exposure and temperatures similar to those in Iraq.

Additionally, mechanical failures (e.g. broken glasses, broken/cracked cells) were prevalent especially among the modules in Baghdad that had been in operation for 8 years. We attribute this to mainly poor handling of modules during installation, poor installation of modules and lack of experience in operation and maintenance activities. For example, Fig. 4 shows the dust cleaning process and how the module can be prone to mechanical stresses by impact (i.e., a cleaning brush hitting the module or someone stepping on the module).

Table 4
Failure modes observed during the visual inspection at the site in Baghdad and Basrah. At Baghdad the inspection was done on October 5, 2020 and at the site in Basra the inspection was carried out on 14.10.2020.

Baghdad	Basrah
o Delamination. o Broken glass by impact. o Encapsulate discoloration and slight browning in the centre of the cell. o Failures caused by and/or during the installation. o Broken/cracked cells and snail trails. o Cells browning.	o Delamination. o EVA browning. o Cell damage by impact. o Dust and birds' droppings. o Modules' surface abrasion due to dust accumulation.

3.1.2. Electrical performance characterization

Fig. 5, shows the degradation of electrical parameters in percentage after 8 years of exposure in Baghdad and after 3.5 years of exposure in Basrah. Additionally, Fig. 6, shows boxplots of the evaluated annual degradation rates for Baghdad and Basrah separately and Baghdad and Basrah combined. Note that in the boxplot for Baghdad, module M1 was not considered because we assumed that such strong cell cracks/breakage could not be due to ageing but instead to handling issues and including it in evaluating the degradation rates would lead to unrealistic conclusions. Therefore, the data plotted and used to evaluate the median degradation rates is for only modules M2 and M3 for Baghdad. All modules were considered for Basrah.

The median degradation rate of Pmax is 2.6 %/year in Baghdad and 0.91 %/year in Basrah. Given that manufacturers provide warranties between 25 and 30 years, the degradation rates to achieve these warranties should not be more than 0.8–0.67 %/year respectively. The degradation rate of 2.6 %/year and 0.91 %/year is equivalent to 7.7 and 21.5 years respectively, which is below the manufacturer's warranty. However, the evaluated degradation rate for Basrah is consistent with what many authors have reported in hot and dry (desert) climates where the degradation rates of power output are above the manufacturer's specifications [5,14,24,63]. Nevertheless, it is important to emphasize that the primary focus of this analysis is not to primarily compare the degradation rates in the two locations, as the modules are sourced from different manufacturers and have been operational for varying periods. Rather, the objective is to assess how the performance of the modules has degraded due to the observed failure modes in each location.

3.1.3. Electroluminescence imaging

Fig. 7, shows the EL images of the modules installed in Baghdad and Basrah. All the three modules from Baghdad exhibited severe cracked or broken cells with all the cells in module M1 completely broken. Indeed, this aligns with the notably high degradation rates observed in the Baghdad modules. When attempting to correlate the cracked or broken cells with the electrical parameters, it was observed that apart from module M1 which was significantly affected by broken cells, the Imax and Isc showed an improvement for modules M2 and M3 despite the presence of cracked or broken cells. This observation requires further investigation as direct interpretation is challenging. Moreover, a different trend is observed for modules in Basrah where modules M2 and M4 exhibiting more pronounced cell cracks showed higher Imax degradation compared to other modules.

It's worth noting that the strong effect of cell breakage/crack observable in the modules installed in Baghdad, cannot solely be attributed to ageing. But is likely attributable to bad practices in installation and during O&M activities.

3.1.4. Degradation rates prediction

We utilized the degradation rate models outlined in section 2.2 to estimate the degradation rates across Iraq using processed ERA5 data described in section 1.2. Fig. 8, shows the simulated degradation rates for specific degradation mechanisms as well as the total or combined degradation rates. Several observations arise from this simulation:

Comparing the three degradation mechanisms, simulations indicate

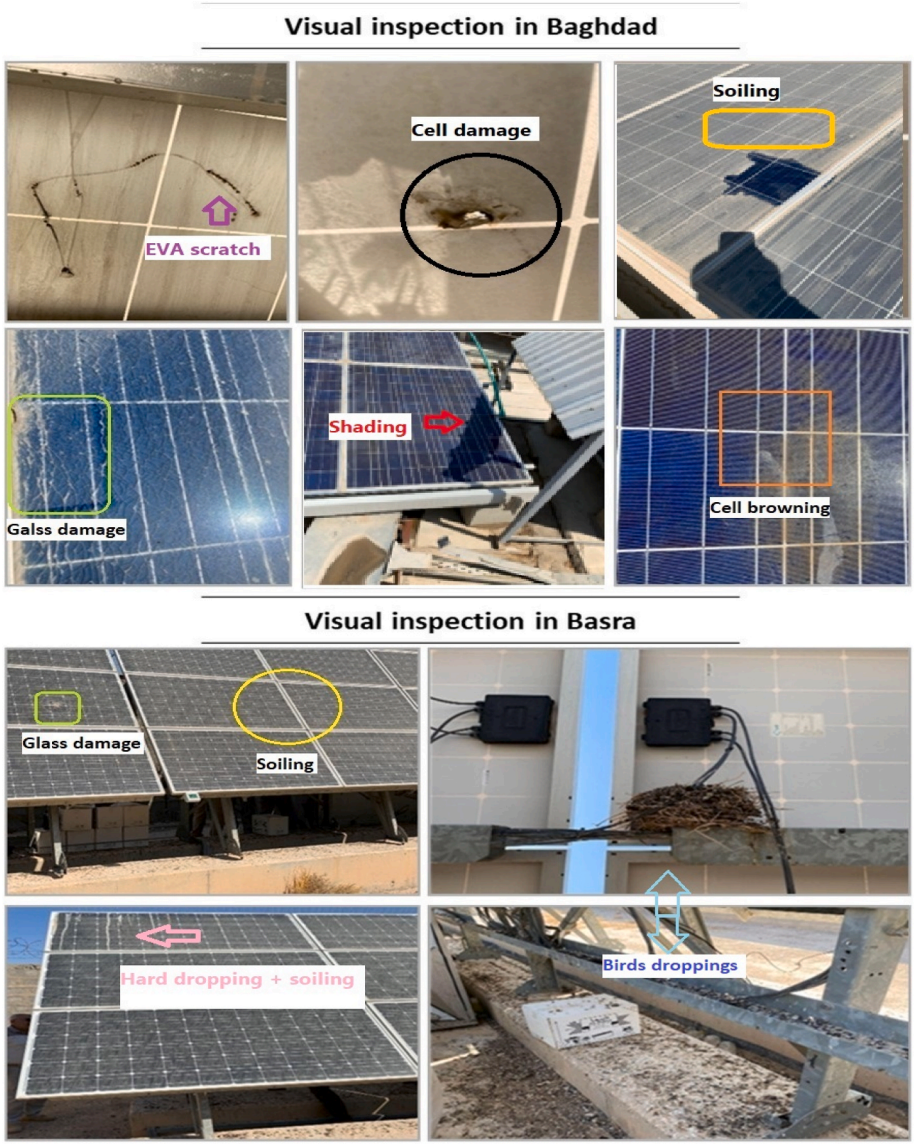

Fig. 3. Visual inspection of modules installed in Baghdad and Basrah.

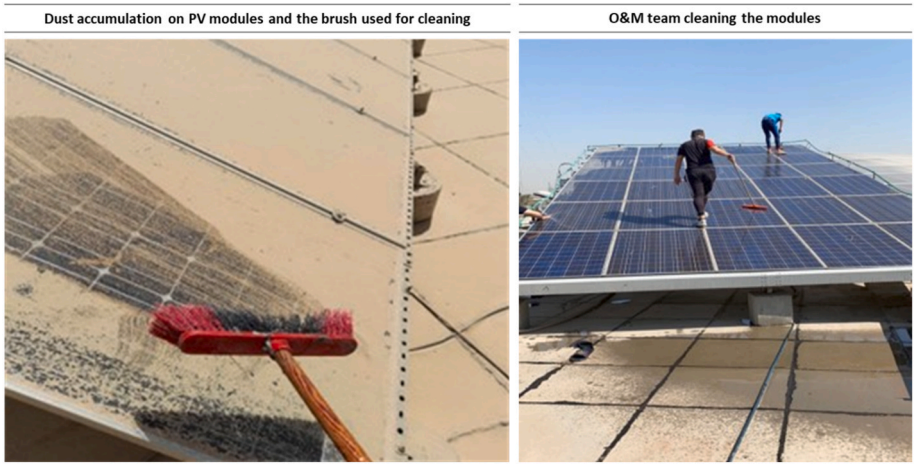

Fig. 4. Dust accumulation on PV modules installed in Iraq and the cleaning process currently used.

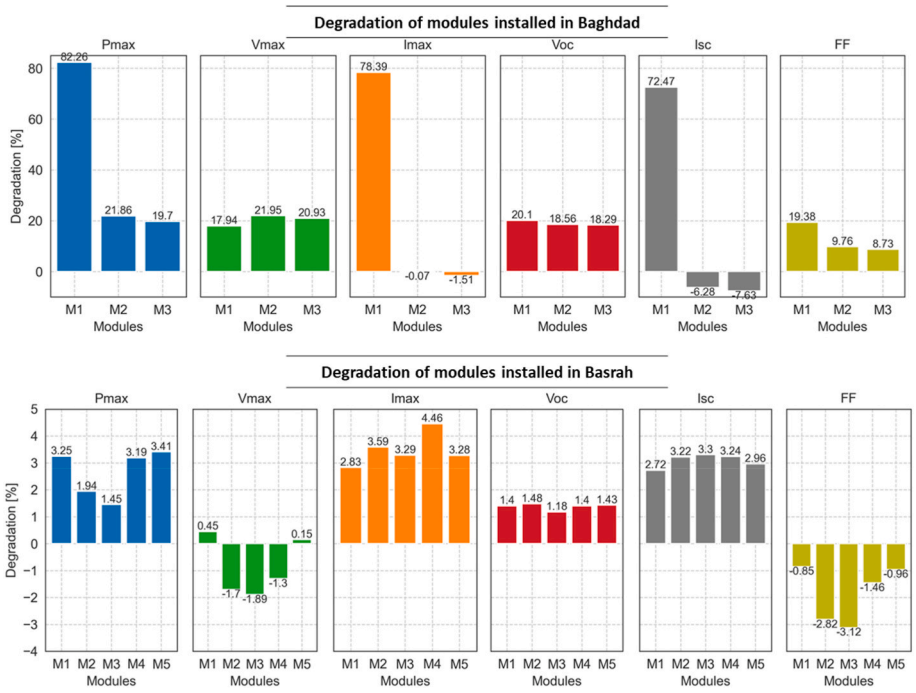

Fig. 5. Evaluated degradation of different electrical parameters for modules installed in Baghdad and Basrah based on the datasheet values. Negative values mean improvement in performance.

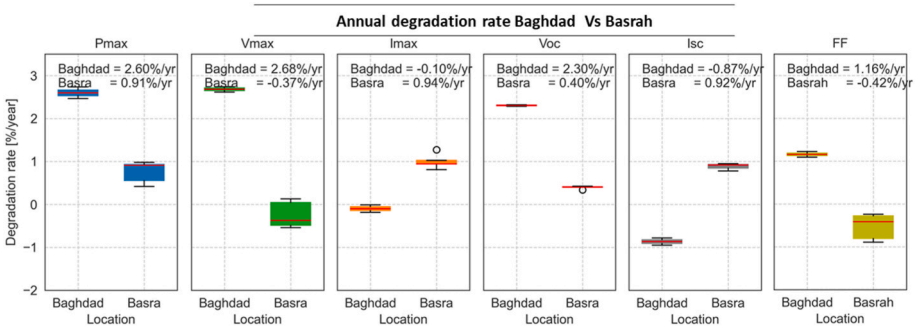

Fig. 6. Boxplots of the annual degradation rates of different electrical parameters for module installed in Baghdad and Basrah. The values shown in the figures are the median values.

that thermomechanical degradation is the most influential mechanism followed by photodegradation, with variations observed across different regions of Iraq. The degradation due to Hydrolysis appears to be the least significant, averaging less than 0.1 %/year throughout the country. This can be explained by the low annual average relative humidity typically below 50 % in most parts of the country (see Fig. 1). Even in regions with relative humidity exceeding 50 % module temperatures are relatively low thus reducing the acceleration of the hydrolysis mechanism. Excluding operational issues, the simulation trends are consistent with the field observations that thermomechanical and photodegradation effects (e.g., delamination, cell cracks and browning as observed in visual inspection and EL images) are the predominant failure mechanisms, which is also consistent with the literature [62].

Comparing the simulated degradation rate in Baghdad and Basrah, a higher degradation rate is predicted in Basrah (1.0∓ 0.1 %/year) compared to Baghdad (0.9∓ 0.1 %/year). While this may appear inconsistent with the degradation rates evaluated from the field in Baghdad, however, modules in Baghdad seem appear to have experienced more failures due to bad practices during O&M activities such as broken glass or cells by impact more than failure modes by ageing. Excluding these effects could yield a more accurate comparison. The predicted degradation rate in Basrah (1.0∓ 0.1 %/year) is comparable to what is evaluated in the field and given that these modules experience fewer operational failures the degradation field degradation can be comparable.

It's important to note that the model was parameterized assuming start-of-the-art PV modules with a good bill of material. This means that the degradation rates for older or bad quality PV modules could be relatively higher than what is presented in this study. We assumed that the industry is moving towards more reliable PV modules and the predicted degradation rates apply to current and future PV modules. Of course, variations due to installation (i.e., building integrated PV – BIPV Vs open rack, tilt angle etc.) and variations in the microclimate conditions around the PV modules are expected to affect the degradation rates even in the same geographical locations. We intend to further explore these effects comprehensively in a separate study. Furthermore, it's important to highlight that even these modules will undergo a certain degree of unpredictable deterioration from factors beyond material quality. The assessment solely addresses gradual degradation and doesn't account for unforeseeable events like hail impact, fire, and similar occurrences.

Based on the modelled total degradation rate, we propose 4 degra-

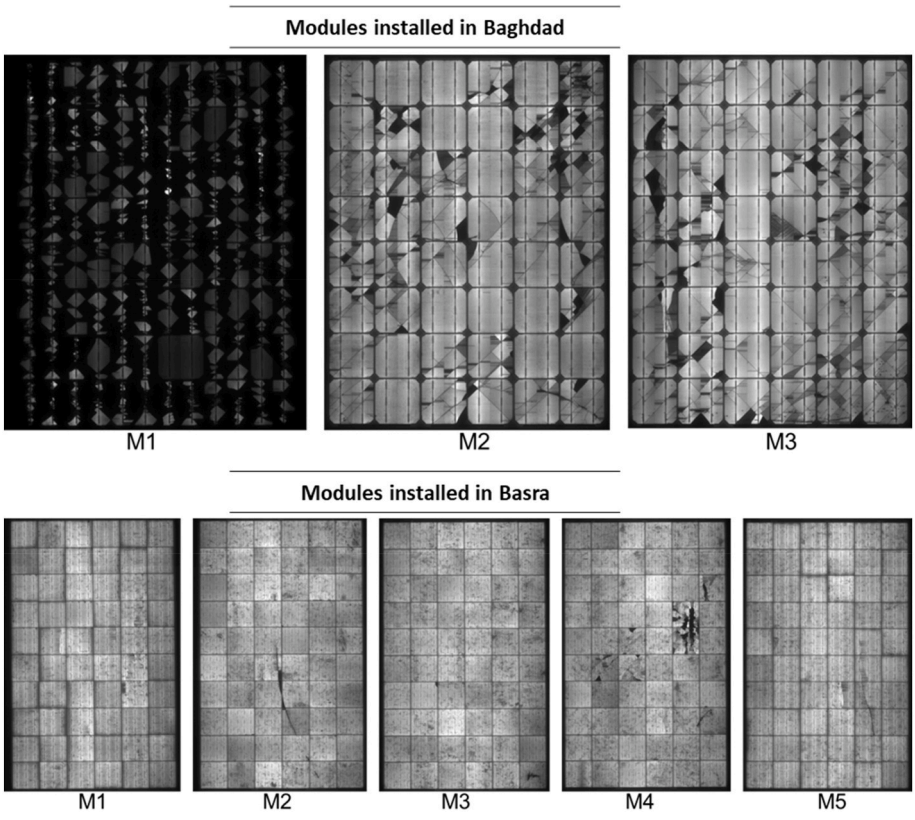

Fig. 7. EL images of the modules installed in Baghdad and Basrah.

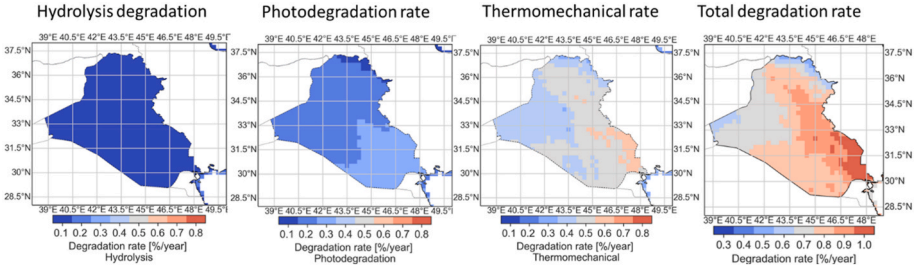

Fig. 8. Simulated degradation rates by degradation mechanism and combined (total) degradation rate across Iraq.

dation zones: Z1, Z2, Z3 and Z4 representing low, moderate, high, and extreme degradation rates respectively (see Fig. 9), for simplicity. This categorization aims to accommodate the variability of the input parameters and variables used in degradation rate predictions over the years. To establish these four zones, we categorized the degradation rates into specified ranges as follows: Z1 ($DR < 0.7\%/year$), Z2 ($0.7 > DR \leq 0.8\%/year$), Z3 ($0.8 > DR \leq 0.9\%/year$) and Z4 ($DR > 0.9\ \%/year$). The distribution of degradation rates across the four zones is shown in the violin plots in Fig. 10. For each of the four zones we recommended utilizing the mean values (as shown on the map in Fig. 9) with uncertainty range of $\mp$ 0.1 %/year.

Considering both lifetime and warranty implications, even when assuming the start-of-the-art PV modules in our simulation, only zone Z1 is within the 30-year warranty threshold where the maximum degradation rate threshold must not exceed 0.67 %/year. Zone Z2 falls within the 25-year warranty where the degradation rate is required to be less than 0.8 %/year. Zones Z3 and Z4 all exhibit degradation rates below the 25-year warranty threshold.

3.2. Lifetime energy yield prediction

3.2.1. Lifetime energy yield prediction without soiling degradation

The primary aim of evaluating the lifetime energy yield is to assess potential trade-offs between locations characterized by higher irradiance but shorter lifetime and those with lower irradiance but with longer lifetime. To achieve this, we selected eight locations as shown in Table 5, based on the optimal annual plane of array irradiance and degradation rates as shown in Fig. 12.

Fig. 11, shows the annual energy yield and PR for the simulated locations. Analysis of the simulated trends in annual energy yield reveals that, within the initial 20 years of the PV system lifetime, location L2 exhibits comparatively lower energy production compared to L3, L6 and L7. However, beyond 20 years of operation, it starts to outperform locations L3, L6 and L7 because of its lower degradation rate compared to these locations. The PR trends highlight the four degradation rate zones, that is, the lower degradation rate zones (L1, L2, L4, L5) demonstrate higher PR, while the zone with the highest degradation rate, L7, exhibits the lowest PR.

Fig. 12, shows the simulated lifetime energy yield in kWh/kWp in locations L1 – L8. Simulations show that L4 and L5 have the highest

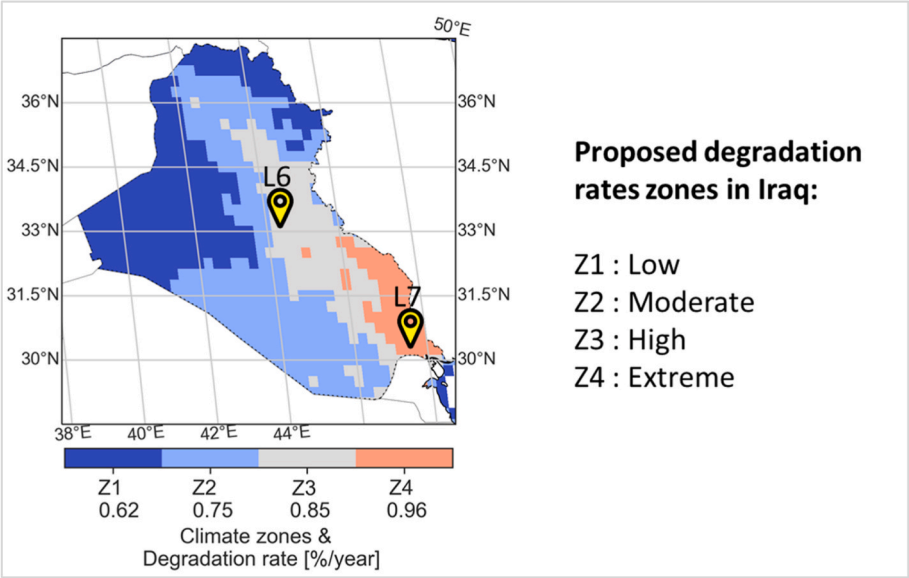

Fig. 9. Proposed degradation rate zones and recommended degradation rates for the different parts of Iraq. L6 and L7 are highlighted locations for Baghdad and Basrah respectively.

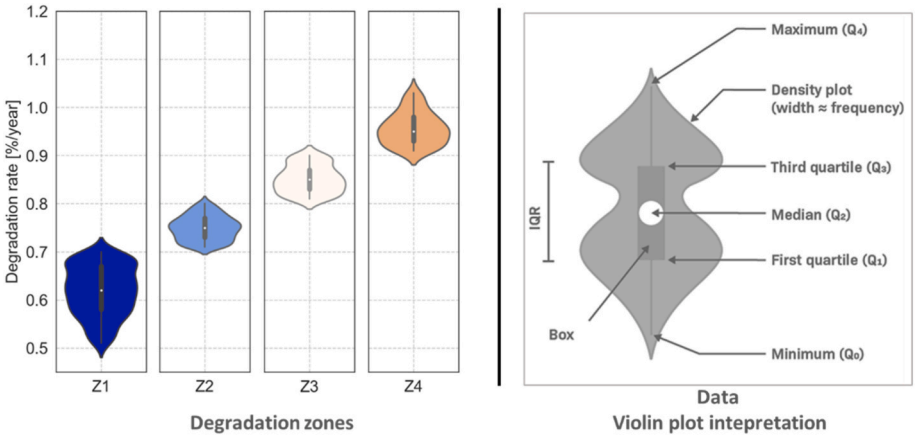

Fig. 10. Violin plots showing the distribution of degradation rates in the four zones (left) and the guide to the interpretation of the violin plot (right).

Table 5
Selected locations for energy yield simulation.

Map showing the locations	Location (Lat./Lon.)	DR zone (DR [%/year])
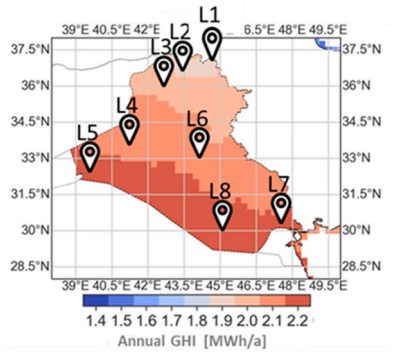	L1 (37.0°/ 44.5°)	Z1(0.62)
	L2 (36.5°/ 43.5°)	Z1 (0.62)
	L3 (36.0°/ 42.5°)	Z2 (0.75)
	L4 (33.5°/ 41.0°)	Z1 (0.62)
	L5 (32.5°/ 39.5°)	Z1 (0.62)
	Baghdad L6 (33.0°/ 44.4°)	Z3 (0.85)
	Basrah L7 (30.2°/ 47.5″)	Z4 (0.96)
	L8 (30.0°/ 45.0°)	Z2 (0.75)

lifetime energy yield, which is not surprising given the low degradation rates and higher annual irradiance in the plane of the array received in these two locations.

The expected trade-offs between locations with higher irradiance and shorter lifetime versus locations with low irradiance and longer lifetime are observed when comparing the lifetime energy yield of location L1 with L3, L6, L7 and L8. It is visible that despite the low irradiance levels received by the modules in L1 they still outperform locations L3, L6, L7, and L8 in terms of lifetime energy yield, thanks to the low degradation rate in L1 which extends the lifetime of PV modules.

Fig. 13, illustrates discrepancies in lifetime energy yield estimates across eight locations when assuming a fixed 30-year lifetime compared to climate-based degradation rates. In locations L1, L2, L4, and L5, using a fixed lifetime underestimates yield by approximately 9.7 %, while in L3, L6, L7, and L8, it overestimates by varying percentages ranging from~10.5 % tõ31.1 %. This suggests that PV project evaluations should consider climate-specific degradation rates rather than fixed degradation rate assumptions across locations.

3.3. Soiling loss/degradation prediction

To simulate the soiling losses, we used the inputs specified in Table 3.

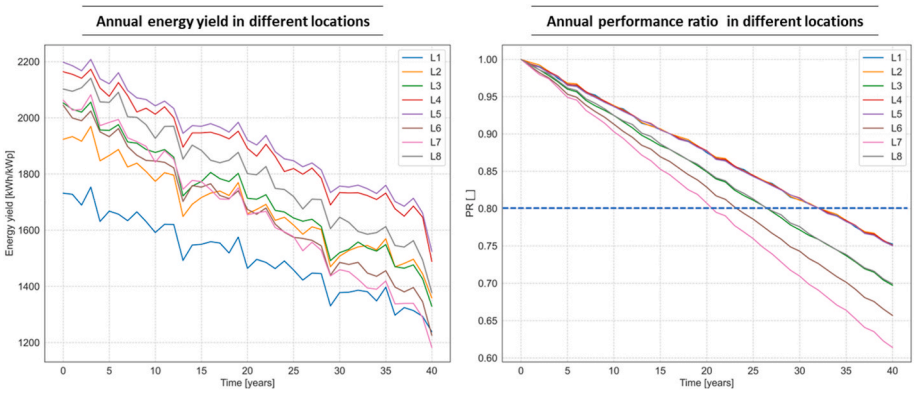

Fig. 11. Simulated annual energy yield and renormalized performance ratio (PR) in the selected locations. The dashed horizontal blue line indicated the threshold the PV lifetime was defined.

Location	L1	L2	L3	L4	L5	L6	L7	L8
DR [%/year]	0.62	0.62	0.75	0.62	0.62	0.85	0.96	0.75
FT [years]	32	32	26	32	32	23	20	26
Gpoa [kWh/m²/a]	1939.78	2215.97	2318.15	2416.15	2444.49	2341.5	2393.65	2428.3
Yield_FT [kWh/kWp]	49674.47	55433	47921.2	62389.3	63376.3	42186.7	37679.7	50184.5
Yield_30 [kWh/kWp]	45246.01	50547.8	53524	56806	57698.2	51652.9	56033	54644.6
Tmod [°C]	31.79	39.41	37.5	34.9	34.01	40.94	41	38.61
Tmax [°C]	60.61	67.57	63.85	58.3	58.85	64.9	65.31	62.11

Fig. 12. Simulated lifetime energy yield using climate-based lifetime (Yield_FT) and assuming a fixed 30-year lifetime (Yield_30) in the selected locations (L1 – L8). The figure also shows other variables that influence the energy yield as a guide for results analysis.

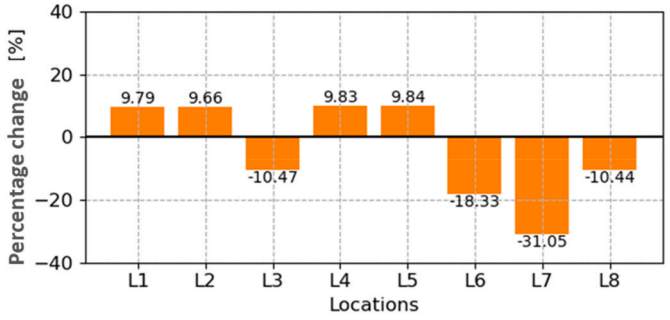

Fig. 13. Percentage change of predicted lifetime energy yield assuming the same degradation rate (lifetime of 30 years) and when evaluated with degradation rates depending on climate zones. (Positive means under prediction and negative means overprediction).

Fig. 14, shows the annual average rainfall days across the eight locations with rainfall exceeding 20 mm. Based on 15-years timeseries dataset, it is evident that generally experiences less than 4 days of rainfall exceeding 20 mm on average, indicating minimal benefit from PV cleaning by rainfall.

Fig. 15, shows an example of the daily PR evaluated with and without soiling plotted together with the rainfall data. From the figure, it is seen that for days with daily rainfall exceeding 20 mm, the daily PR with and without soiling remains similar until the next 10 days (considered as grace period) indicating self-cleaning of the modules by rainfall.

The soiling loss assessment was carried out for two main objectives: (1) to evaluate the variations in lifetime energy yield predictions with and without considering soiling losses, and (2) to assess the benefits of natural cleaning by rainfall. The results for both objectives are summarized in Fig. 16 and can be interpreted as:

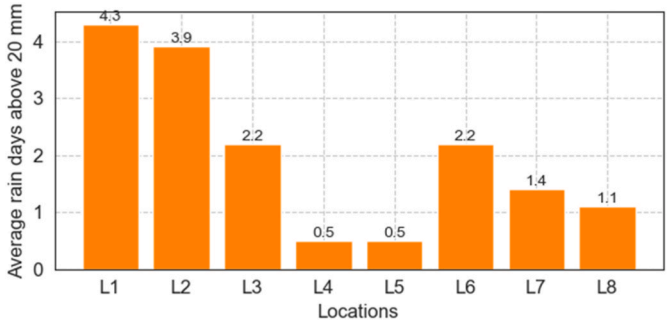

Fig. 14. Average rain days in a year with rainfall above 20 mm. Average plotted using 15 years of data from 2005 to 2020.

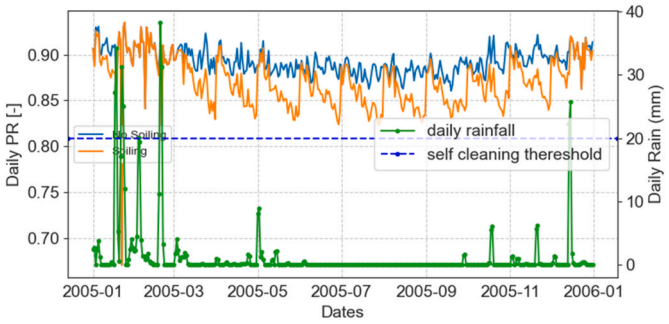

Fig. 15. Daily performance ratio without soiling (in blue) and with soiling (in orange). In green is the daily rainfall data and the dashed horizontal blue line indicates the cleaning threshold (i.e., daily rainfall equal or above 20 mm).

Soiling effect: location L1

Cleaning time [Months]	1	2	3	4	5	6
0.2 [%/day]	2.74%	5.34%	7.72%	9.95%	12.14%	13.02%
0.3 [%/day]	4.17%	8.23%	12.04%	15.71%	19.39%	20.88%
0.4 [%/day]	5.64%	11.29%	16.73%	22.10%	27.64%	29.93%
0.5 [%/day]	7.14%	14.15%	21.82%	29.24%	37.12%	40.04%

Soiling effect: location L4

Cleaning time [Months]	1	2	3	4	5	6
0.2 [%/day]	3.04%	6.22%	9.52%	12.98%	16.40%	19.98%
0.3 [%/day]	4.63%	9.62%	15.00%	20.83%	26.80%	33.30%
0.4 [%/day]	6.27%	13.26%	21.05%	29.84%	39.24%	49.94%
0.5 [%/day]	7.96%	17.14%	27.77%	40.31%	54.38%	69.80%

Fig. 16. Simulated percentage change of lifetime energy yield prediction with and without soiling for location L1 (with 4.3 rainfall days exceeding 20 mm per year) and location L4 (with 0.5 rainfall days exceeding 20 mm per year) and at different soiling rates (0.2 %/day to 0.5 %/day).

- o Soiling losses can vary significantly, ranging from 2.74 % to 69.80 % depending on the soiling loss rate, location, and manual cleaning schedules. This also implies that without considering the soiling loss, lifetime yield predictions are overestimated within the same range.
- o The self-cleaning or natural by rainfall has demonstrates a positive impact as evidenced by comparing the percentage differences evaluated for location L1, which experiences more rainfall days annually, with location L4. At the same soiling loss rates the soiling loss is more pronounced in location L4 compared to location L1 (i.e., the maximum evaluated loss for L4 is approximately 70 % compared to 40 % for L1).

It should be noted that, although other types of soiling like bird droppings were observed, we assumed soiling by dust accumulation in our analysis, presuming consistent dust characteristics across all locations. This assumption was made due to the difficulty in quantifying and extrapolating soiling caused by bird droppings to other locations, given limited data availability. Additionally, the soiling model utilized in the study was not validated for soiling caused by bird droppings.

4. Conclusion

The increasing deployment of PV systems globally, especially in developing nations to solve their energy needs, represents a sustainable solution. However, the lack of comprehensive data on PV performance and reliability in many of these nations introduces uncertainties when assessing the viability of PV projects. For example, countries like Iraq, have a promising potential for PV energy generation due to the amount of solar energy that the country receives per year. However, at the same time, the country is also characterized by harsh climatic conditions such as higher temperatures, high UV doses and frequent soiling which hinder the performance and reliability of PV. It is most likely that modules installed in these harsh environments experience different failure modes and have a reduced lifetime. However, the most prevalent failure modes, the extent of the PV module's lifetime reduction compared to other locations, and potential trade-offs in lifetime energy production between high irradiance regions with a shorter lifetime and low irradiance areas with longer lifetime remain uncertain. In this study, we analyse the degradation of operational PV modules in Basrah and Baghdad that have been under field exposure for a period of 3 and 8 years respectively to assess the prevalent failure modes. In the study, we also employ degradation rate and soiling loss models to simulate degradation rates and lifetime energy yield for PV modules across Iraq.

By using the field data from the two locations, we have identified that the most common failure modes experienced by the modules installed in Iraq are: solder bond fatigue, glass/cell crack and breakage impact, delamination, and discoloration. We assessed the electrical performance degradation based on the datasheet values, revealing median Pmax degradation rates of 0.91 % and 2.6 % per year in Basrah and Baghdad, respectively, with a combined median degradation rate of 0.93 % per year across both locations. One key observation is that the evaluated performance degradation rate, especially in Baghdad, is not only linked to ageing but also to poor O&M practices which leads to acceleration of module failure.

Using climate-based degradation models, we simulated degradation rates across all regions in Iraq and proposed four degradation zones: Z1 (low), Z2(moderate), Z3(high) and Z4(extreme) with medium degradation rates of 0.62 %/year, 0.75 %/year, 0.85 %/year, and 0.96 %/year respectively. Using these degradation rates, we assessed the trade-offs in lifetime energy yield, demonstrating that modules installed in locations with lower irradiance, but longer lifetime generate more energy over their lifetime compared to those in locations with higher irradiance but shorter lifetime. We also examined the effects of using a uniform lifetime in lifetime energy predictions across the country, revealing potential overestimations of up to 31.05 % in certain areas, which could lead to erroneous financial decisions. Subsequently, future studies aim to evaluate the financial impacts of such under/overestimations.

Furthermore, we assessed the soiling losses by simulating different scenarios. We found out that the soiling losses in Iraq could be as high as 70 % depending on the location and the cleaning schedule. We observed minimal influence of self-cleaning due to limited rainfall across the country, although distinctions were noticeable when comparing regions

with varying rainfall levels. It's important to note that our analysis solely considered the influence of rainfall due to limitations in the soiling model utilized in this study and available data. Future endeavours

will expand soiling loss modelling to incorporate factors such as tilt angle, wind speed, and soiling particle characteristics, which also influence soiling losses.

CRediT authorship contribution statement

Mohammed Adnan Hameed: Writing – original draft, Visualization, Validation, Software, Investigation, Data curation. **Ismail Kaaya:** Software, Data curation. **Mudhafar Al-Jbori:** Investigation, Data curation. **Qais Matti:** Supervision, Investigation. **Roland Scheer:** Supervision. **Ralph Gottschalg:** Supervision.

Declaration of competing interest

The authors declare that they have no known competing financial interests or personal relationships that could have appeared to influence the work reported in this paper.

Acknowledgements

This study received no funding, and the authors declare no conflict of interest. The authors would like to acknowledge Julian Ascencio-Vásquez for providing processed climatic data used in this study for the mapping. Also, Majid Hamadi Al-Seadi in the Ministry of Oil-Iraq, for the support provided during in the site inspection.

References

[1] Iraq's Energy Sector: A Roadmap to a Brighter Future – Analysis," IEA. Accessed: July. 10, 2023. [Online]. Available: https://www.iea.org/reports/iraqs-energy-sector-a-roadmap-to-a-brighter-future.
[2] Iraq - Countries & Regions," IEA. Accessed: July. 17, 2023. [Online]. Available: https://www.iea.org/countries/iraq.
[3] Iraq needs renewables, but they won't solve its power problems without broader reforms," Middle East Institute. Accessed: July. 17, 2023. [Online]. Available: https://www.mei.edu/publications/iraq-needs-renewables-they-wont-solve-its-power-problems-without-broader-reforms.
[4] S. Rai-Roche, "TotalEnergies agrees to build second 1GW solar plant in Iraq," PV Tech. Accessed: July. 10, 2023. [Online]. Available: https://www.pv-tech.org/totalenergies-agrees-to-build-second-1gw-solar-plant-in-iraq/.
[5] D.C. Jordan, S.R. Kurtz, K. VanSant, J. Newmiller, Compendium of photovoltaic degradation rates, Prog. Photovoltaics Res. Appl. 24 (7) (2016) 978–989, https://doi.org/10.1002/pip.2744.
[6] H. Al-Lami, N.N. Al-Mayyahi, Q. Al-Yasiri, R. Ali, A. Alshara, Performance enhancement of photovoltaic module using finned phase change material panel: an experimental study under Iraq hot climate conditions, Energy Sources, Part A Recovery, Util. Environ. Eff. 44 (3) (Sep. 2022) 6886–6897, https://doi.org/10.1080/15567036.2022.2103601.
[7] M. Al-Damook, K. Waleed Abid, A. Mumtaz, D. Dixon-Hardy, P.J. Heggs, M. Al Qubeissi, Photovoltaic module efficiency evaluation: the case of Iraq, Alex. Eng. J. 61 (8) (Aug. 2022) 6151–6168, https://doi.org/10.1016/j.aej.2021.11.046.
[8] M.J. Yaseen, N.K. Kasim, A.F. Atwan, Prediction of the Performance of a Solar PV System in Baghdad, Iraq, vol. 2322, Aug. 2022 012079, https://doi.org/10.1088/1742-6596/2322/1/012079.
[9] D. Atsu, I. Seres, M. Aghaei, I. Farkas, Analysis of long-term performance and reliability of PV modules under tropical climatic conditions in sub-Saharan, Renew. Energy 162 (Dec. 2020) 285–295, https://doi.org/10.1016/j.renene.2020.08.021.
[10] C. Baldus-Jeursen, A. Côté, T. Deer, Y. Poissant, Analysis of photovoltaic module performance and life cycle degradation for a 23 year-old array in Quebec, Canada, Renew. Energy 174 (Aug. 2021) 547–556, https://doi.org/10.1016/j.renene.2021.04.013.
[11] D. Hassan Daher, L. Gaillard, C. Ménézo, Experimental assessment of long-term performance degradation for a PV power plant operating in a desert maritime climate, Renew. Energy 187 (Mar. 2022) 44–55, https://doi.org/10.1016/j.renene.2022.01.056.
[12] A. Ameur, A. Berrada, A. Bouaichi, K. Loudiyi, Long-term performance and degradation analysis of different PV modules under temperate climate, Renew. Energy 188 (Apr. 2022) 37–51, https://doi.org/10.1016/j.renene.2022.02.025.
[13] S.K. Singh, N. Chander, Mid-life degradation evaluation of polycrystalline Si solar photovoltaic modules in a 100 kWp grid-tied system in east-central India, Renew. Energy 199 (Nov. 2022) 351–367, https://doi.org/10.1016/j.renene.2022.09.013.
[14] B. Aboagye, S. Gyamfi, E.A. Ofosu, S. Djordjevic, Characterisation of degradation of photovoltaic (PV) module technologies in different climatic zones in Ghana, Sustain. Energy Technol. Assessments 52 (Aug. 2022) 102034, https://doi.org/10.1016/j.seta.2022.102034.
[15] D.A. Quansah, M.S. Adaramola, Assessment of early degradation and performance loss in five co-located solar photovoltaic module technologies installed in Ghana using performance ratio time-series regression, Renew. Energy 131 (Feb. 2019) 900–910, https://doi.org/10.1016/j.renene.2018.07.117.
[16] A. Louwen, S. Lindig, G. Chowdhury, D. Moser, Climate- and technology-dependent performance loss rates in a large commercial photovoltaic monitoring dataset, Sol. RRL 8 (5) (2024) 2300653, https://doi.org/10.1002/solr.202300653.
[17] D.C. Jordan, et al., Photovoltaic fleet degradation insights, Prog. Photovoltaics Res. Appl. 30 (10) (2022) 1166–1175, https://doi.org/10.1002/pip.3566.
[18] M. Piliougine, P. Sánchez-Friera, G. Petrone, F.J. Sánchez-Pacheco, G. Spagnuolo, M. Sidrach-de-Cardona, Analysis of the degradation of amorphous silicon-based modules after 11 years of exposure by means of IEC60891:2021 procedure 3, Prog. Photovoltaics Res. Appl. 30 (10) (2022) 1176–1187, https://doi.org/10.1002/pip.3567.
[19] H. Saad, A.I. Al-Tmimi, Simulating the performance of solar panels in Iraq, J. Appl. Adv. Res. (Jan. 2019) 6–10, https://doi.org/10.21839/jaar.2019.v4i1.264.
[20] M.T. Chaichan, et al., Sand and dust storms' impact on the efficiency of the photovoltaic modules installed in Baghdad: a review study with an empirical investigation, Energies 16 (9) (Jan. 2023) 9, https://doi.org/10.3390/en16093938.
[21] G. Jendar, L. Al-Rubaye, Q. Hassan, B. Ceran, A. Mohamad, Experimental investigation of soiling and temperature impact on PV power degradation: north east-Iraq as A case study, Diyala J. Eng. Sci. 15 (Jan. 2022) 10–26.
[22] M.T. Chaichan, H.A. Kazem, A.H.A. Al-Waeli, K. Sopian, The effect of dust components and contaminants on the performance of photovoltaic for the four regions in Iraq: a practical study, Renew. Energy Environ. Sustain 5 (2020) 3, https://doi.org/10.1051/rees/2019009.
[23] A. Al-Ammri, A. Ghazi Abdulshaheed, F. Mustafa Al-attar, Dust Effects on the Performance of PV Street Light in Baghdad City, 2013, p. 22, https://doi.org/10.1109/IRSEC.2013.6529687.
[24] R. Dubey, et al., Comprehensive study of performance degradation of field-mounted photovoltaic modules in India, Energy Sci. Eng. 5 (1) (2017) 51–64, https://doi.org/10.1002/ese3.150.
[25] T. Karin, C. Jones, A. Jain, Photovoltaic Degradation Climate Zones, Jun. 2019, https://doi.org/10.1109/PVSC40753.2019.8980831.
[26] M. Aghaei, et al., Review of degradation and failure phenomena in photovoltaic modules, Renew. Sustain. Energy Rev. 159 (May 2022) 112160, https://doi.org/10.1016/j.rser.2022.112160.
[27] J. Ascencio-Vásquez, I. Kaaya, K. Brecl, K.-A. Weiss, M. Topič, Global climate data processing and mapping of degradation mechanisms and degradation rates of PV modules, Energies 12 (24) (Jan. 2019) 4749, https://doi.org/10.3390/en12244749.
[28] D.C. Jordan, S.R. Kurtz, Photovoltaic degradation rates—an analytical review, Prog. Photovoltaics Res. Appl. 21 (1) (2013) 12–29, https://doi.org/10.1002/pip.1182.
[29] R. Dubey, et al., Comprehensive study of performance degradation of field-mounted photovoltaic modules in India, Energy Sci. Eng. 5 (1) (2017) 51–64, https://doi.org/10.1002/ese3.150.
[30] J.-F. Lelièvre, et al., Desert label development for improved reliability and durability of photovoltaic modules in harsh desert conditions, Sol. Energy Mater. Sol. Cells 236 (Mar. 2022) 111508, https://doi.org/10.1016/j.solmat.2021.111508.
[31] S. Gyamfi, B. Aboagye, F. Peprah, M. Obeng, Degradation analysis of polycrystalline silicon modules from different manufacturers under the same climatic conditions, Energy Convers. Manag. X 20 (Oct. 2023) 100403, https://doi.org/10.1016/j.ecmx.2023.100403.
[32] I. Kaaya, J. Ascencio-Vásquez, I. Kaaya, J. Ascencio-Vásquez, Photovoltaic power forecasting methods, in: Solar Radiation - Measurement, Modeling and Forecasting Techniques for Photovoltaic Solar Energy Applications, IntechOpen, 2021, https://doi.org/10.5772/intechopen.97049.
[33] I.T. Horváth, et al., Photovoltaic energy yield modelling under desert and moderate climates: what-if exploration of different cell technologies, Sol. Energy 173 (Oct. 2018) 728–739, https://doi.org/10.1016/j.solener.2018.07.079.
[34] D. Markovics, M.J. Mayer, Comparison of machine learning methods for photovoltaic power forecasting based on numerical weather prediction, Renew. Sustain. Energy Rev. 161 (Jun. 2022) 112364, https://doi.org/10.1016/j.rser.2022.112364.
[35] B. Goss, I.R. Cole, E. Koubli, D. Palmer, T.R. Betts, R. Gottschalg, 4 - modelling and prediction of PV module energy yield, in: N. Pearsall (Ed.), The Performance of Photovoltaic (PV) Systems, Woodhead Publishing, 2017, pp. 103–132, https://doi.org/10.1016/B978-1-78242-336-2.00004-5.
[36] G.P. Smestad, et al., Modelling photovoltaic soiling losses through optical characterization, Sci. Rep. 10 (1) (Jan. 2020) 1, https://doi.org/10.1038/s41598-019-56868-z.
[37] R.K. Jones, et al., Optimized cleaning cost and schedule based on observed soiling conditions for photovoltaic plants in Central Saudi Arabia, IEEE J. Photovoltaics 6 (3) (May 2016) 730–738, https://doi.org/10.1109/JPHOTOV.2016.2535308.
[38] R. Shenouda, M.S. Abd-Elhady, H.A. Kandil, A review of dust accumulation on PV panels in the MENA and the Far East regions, J. Eng. Appl. Sci. 69 (1) (Jan. 2022) 8, https://doi.org/10.1186/s44147-021-00052-6.
[39] M. Coello, L. Boyle, Simple model for predicting time series soiling of photovoltaic panels, IEEE J. Photovoltaics 9 (5) (Sep. 2019) 1382–1387, https://doi.org/10.1109/JPHOTOV.2019.2919628.

[40] A. Kimber, L. Mitchell, S. Nogradi, H. Wenger, The effect of soiling on large grid-connected photovoltaic systems in California and the southwest region of the United States, in: 2006 IEEE 4th World Conference on Photovoltaic Energy Conference, May 2006, pp. 2391–2395, https://doi.org/10.1109/WCPEC.2006.279690.
[41] Climate reanalysis | Copernicus." Accessed: January. 30, 2022. [Online]. Available: https://climate.copernicus.eu/climate-reanalysis.
[42] PVGIS data sources & calculation methods." Accessed: July. 11, 2023. [Online]. Available: https://joint-research-centre.ec.europa.eu/photovoltaic-geographical-information-system-pvgis/getting-started-pvgis/pvgis-data-sources-calculation-methods_en.
[43] Copernicus Climate Change Service, Precipitation Monthly and Daily Gridded Data from 1979 to Present Derived from Satellite Measurement. Copernicus Climate Change Service (C3S) Climate Data Store (CDS: DOI: 10.24381/cds.C14d9324, 2021 [Online]. Available: https://cds.climate.copernicus.eu/cdsapp#!/dataset/10.24381/cds.c14d9324?tab=overview. (Accessed 12 July 2023).
[44] JRC Photovoltaic Geographical Information System (PVGIS) - European Commission." Accessed: April. 3, 2023. [Online]. Available: https://re.jrc.ec.europa.eu/pvg_tools/en/#TMY.
[45] I. Kaaya, M. Köhl, A. Mehilli, S. de C. Mariano, K.A. Weiss, Modeling outdoor Service lifetime prediction of PV modules: effects of combined climatic stressors on PV module power degradation, IEEE J. Photovoltaics 9 (2019) 1105–1112, https://doi.org/10.1002/pip.2793.
[46] I. Kaaya, J. Ascencio-Vásquez, K.-A. Weiss, M. Topič, Assessment of uncertainties and variations in PV modules degradation rates and lifetime predictions using physical models, Sol. Energy 218 (Apr. 2021) 354–367, https://doi.org/10.1016/j.solener.2021.01.071.
[47] I. Kaaya, D. Mansour, P. Gebhardt, K. Weiß, D. Philipp, Modelling and validation of photovoltaic degradation under ultraviolet-damp-heat conditions, in: 2021 IEEE 48th Photovolt, Spec. Conf. PVSC, 2021, https://doi.org/10.1109/PVSC43889.2021.9519050.
[48] scipy.stats.ncf — SciPy v1.11.1 Manual." Accessed: July. 5, 2023. [Online]. Available: https://docs.scipy.org/doc/scipy/reference/generated/scipy.stats.ncf.html.
[49] M. Šúri, T.A. Huld, E.D. Dunlop, H.A. Ossenbrink, Potential of solar electricity generation in the European Union member states and candidate countries, Sol. Energy 81 (10) (Oct. 2007) 1295–1305, https://doi.org/10.1016/j.solener.2006.12.007.
[50] T. Huld, et al., A power-rating model for crystalline silicon PV modules, Sol. Energy Mater. Sol. Cells 95 (12) (2011) 12.
[51] T. Muneer, Solar radiation model for Europe, Build. Serv. Eng. Res. Technol. 11 (4) (Nov. 1990) 153–163, https://doi.org/10.1177/014362449001100405.
[52] D. Faiman, Assessing the outdoor operating temperature of photovoltaic modules, Prog. Photovoltaics Res. Appl. 16 (4) (2008) 307–315, https://doi.org/10.1002/pip.813.
[53] M. Koehl, M. Heck, S. Wiesmeier, J. Wirth, Modeling of the nominal operating cell temperature based on outdoor weathering, Sol. Energy Mater. Sol. Cells 95 (7) (Jul. 2011) 1638–1646, https://doi.org/10.1016/j.solmat.2011.01.020.
[54] I. Kaaya, K.-A. Weiß, Assessing the variations in long-term photovoltaic yield prediction due to solar irradiance and module temperature, in: *Proceedings Of the ISES Solar World Congress 2021*, Virtual, International Solar Energy Society, 2021, pp. 1–6, https://doi.org/10.18086/swc.2021.37.04.
[55] W.F. Holmgren, C.W. Hansen, M.A. Mikofski, Pvlib python: a python package for modeling solar energy systems, J. Open Source Softw. 3 (29) (Sep. 2018) 884, https://doi.org/10.21105/joss.00884.
[56] *Documentation*. pvlib, 2023. Accessed: July. 7, 2023. [Online]. Available: https://github.com/pvlib/pvlib-python.
[57] W. Javed, B. Guo, B. Figgis, L. Martin Pomares, B. Aïssa, Multi-year field assessment of seasonal variability of photovoltaic soiling and environmental factors in a desert environment, Sol. Energy 211 (Nov. 2020) 1392–1402, https://doi.org/10.1016/j.solener.2020.10.076.
[58] M. Theristis, A. Livera, C.B. Jones, G. Makrides, G.E. Georghiou, J.S. Stein, Nonlinear photovoltaic degradation rates: modeling and comparison against conventional methods, IEEE J. Photovoltaics 10 (4) (Jul. 2020) 1112–1118, https://doi.org/10.1109/JPHOTOV.2020.2992432.
[59] I. Kaaya, S. Lindig, K.-A. Weiss, A. Virtuani, M. S. de C. Ortin, and D. Moser, "Photovoltaic lifetime forecast model based on degradation patterns," Prog. Photovoltaics Res. Appl., vol. n/a, no. n/a, doi: 10.1002/pip.3280..
[60] D.C. Jordan, C. Deline, S.R. Kurtz, G.M. Kimball, M. Anderson, Robust PV degradation methodology and application, IEEE J. Photovoltaics 8 (2) (Mar. 2018) 525–531, https://doi.org/10.1109/JPHOTOV.2017.2779779.
[61] Relative Change and Difference," Wikipedia. Jul. 11, 2023. Accessed: July. 18, 2023. [Online]. Available: https://en.wikipedia.org/w/index.php?title=Relative_change_and_difference&oldid=1164822526#cite_note-4.
[62] A. Bouaichi, et al., In-situ evaluation of the early PV module degradation of various technologies under harsh climatic conditions: the case of Morocco, Renew. Energy 143 (Dec. 2019) 1500–1518, https://doi.org/10.1016/j.renene.2019.05.091.
[63] D. H. Daher, M. Aghaei, D. A. Quansah, M. S. Adaramola, P. Parvin, and C. Ménézo, "Multi-pronged degradation analysis of a photovoltaic power plant after 9.5 years of operation under hot desert climatic conditions," Prog. Photovoltaics Res. Appl., vol. n/a, no. n/a, doi: 10.1002/pip.3694..